A two-phase flow model to simulate mold filling and saturation in Resin Transfer Molding

Gascón L.[1], García J.A.[1], LeBel F.[2], Ruiz E.[2], Trochu F.[2]

[1] *Instituto del Diseño para la Fabricación (IDF), Universidad Politécnica de Valencia. Camino Vera s/n, 46022, Valencia (Spain), Email: llgascon@mat.upv.es Tel: +3463879662*

[2] *Chair on Composites of High Performance (CCHP), Mechanical Engineering Department, Center of Research on Polymers and Composites (CREPEC), École Polytechnique de Montréal, Montréal, Canada, H3C 3A7*

Abstract: This paper addresses the numerical simulation of void formation and transport during mold filling in Resin Transfer Molding (RTM). The saturation equation, based on a two-phase flow model resin/air, is coupled with Darcy's law and mass conservation to simulate the unsaturated filling flow that takes place in a RTM mold when resin is injected through the fiber bed. These equations lead to a system composed of an advection-diffusion equation for saturation including capillary effects and an elliptic equation for pressure taking into account the effect of air residual saturation. The model introduces the relative permeability as a function of resin saturation. When capillary effects are omitted, the hyperbolic nature of the saturation equation and its strong coupling with Darcy equation through relative permeability represent a challenging numerical issue. The combination of the constitutive physical laws relating permeability to saturation with the coupled system of the pressure and saturation equations allows predicting the saturation profiles. The model was validated by comparison with experimental data obtained for a fiberglass reinforcement injected in a RTM mold at constant flow rate. The saturation measured as a function of time during the resin impregnation of the fiber bed compared very well with numerical predictions.

Keywords: Resin Transfer Molding; Two-phase flow; Voids; Saturation; Relative permeability

1. Introduction

Liquid Composite Molding (LCM) processes are being increasingly used to manufacture fiber-reinforced composite materials. A good composite product is obtained when the reinforcement is fully impregnated by the resin and properly cured. Due to the double porosity scale of the fibrous reinforcements used in high performance composites, bubbles of different shapes and lengths can be created during mold filling, i.e., mesoscopic voids may appear between the fiber tows and microscopic voids inside the tows [1, 2, 3]. Understanding and preventing the formation of voids is necessary for proper molding of composite parts by LCM. In these processes, saturation is of primary importance in order to predict local defaults. Incomplete saturation may translate into a reduction of mechanical performance and even cause failure of the final product. Hence, mathematical modeling and numerical simulation of saturation are very important issues in LCM because of the aim to optimize the design and manufacture of high performance composites.

Over the past two decades, various models have been proposed to simulate the resin flow through fibrous preforms. A comprehensive review of these methods can be found in [4, 5]. For computational simplicity, the LCM process has been conventionally modeled as a single phase flow, with resin as the only phase. In the case of unidirectional injections at constant flow rate in a rectangular mold, classical models predict a moving linear distribution of pressure in the mold. However, experiments show that a non linear (parabolic) pressure distribution is observed in the local unsaturated zone close to the flow front before the mold is completely filled [6, 7].

The discrepancy between experimental and analytical predictions of the injection pressure versus time has motivated numerous studies on dual scale flows through fibrous reinforcements [8, 9, 10, 11]. In rectilinear and radial flows through a single scale porous medium such as random fiber mats, the inlet pressure increases linearly at constant injection flow rate [9] (see also Fig. 5). However, the inlet pressure drops in time in dual scale porous media such as woven fibrous reinforcements for example. In unsaturated flows through fibrous preforms of double scale porosity, this phenomenon known as pressure drooping [8], has been investigated by several researchers.

On one hand, some authors proposed to incorporate a sink effect on the right hand side of the continuity equation in order to model the unsaturated flow in a double scale porous medium [10, 11]. On the other hand, introducing saturation allows describing in more detail the progressive impregnation of a fibrous preform by a liquid resin. The necessity to account for saturation was clearly demonstrated by De Parseval et al. [9]. Saturation was defined by some investigators as the solution of an advection-diffusion equation [1, 6, 12], where the degree of saturation is advected with the resin velocity. However, the numerical results obtained in Fig. 2 by this approach differ from our experimental observations.

The resin flow in the partially saturated region of the mold cavity can be modeled as a two-phase flow through a porous medium (resin and air). In this case, permeability depends on the degree of saturation of the fibrous reinforcement and describes how each phase flows with respect to the other. However there are few studies in LCM within this multiphase framework. Chui et al. [13] and Nordlund and Michaud [14] were among the first to apply to LCM a two-phase flow model.

Although much progress was made in the last decades on the numerical solution of the formation and transport of voids in LCM, still unresolved issues and limitations remain in the current state of the art. Mathematical modeling and numerical simulation of saturation, coupling the flow equation on pressure and velocity with the transport saturation equation, represent a challenging numerical issue.

The aim of this paper is to derive a new formulation of two-phase flow in LCM to predict void formation and transport during mold filling. The new model proposed in this investigation is based on a fractional flow formulation, with saturation and pressure as primary variables. The solution uses a finite element method for the elliptic pressure equation and a flux limiter technique to approximate the saturation equation. Note that details on the solution algorithm were already described in [15, 16]. As a matter of fact, the comparison of the numerical predictions of saturation with experiments shows that air residual saturation, which can be identified as the air volume contained in immobile bubbles, plays a key role on void formation and transport in LCM.

The rest of the paper is organized as follows. A review on classical two-phase flow models is presented in Section 2. Different ways of coupling the flow, transport and constitutive relations between saturation and relative permeability are described and discussed. Section 3 describes the new mathematical model proposed here to simulate mold filling and saturation in LCM. The boundary value problem is formulated by coupling the hyperbolic transport equation of saturation with the elliptic equation used to calculate the pressure and velocity of the porous flow. Finally, after a short description in Section 4 of the saturation experiments, the predictions of the new model are validated in Section 5 by comparison with the results of injection experiments at constant flow rate [17].

2. Review of two-phase flow and transport models

In multiphase flows through porous media, the permeability of each phase depends on the saturation S of the wetting phase, namely the resin in LCM. Saturation is defined as the ratio of the resin volume over the total pore volume of the engineering fabric. Hence $(1 - S)$ denotes the saturation of the complementary phase, namely the proportion of the pore volume filled with air. Therefore, if two fluids flow within the same porous material, their velocity can be expressed by Darcy's law for each phase *j* as follows:

$$q_j = -\lambda_j\left(S\right)\nabla p_j \tag{1}$$

where q_j is Darcy phase velocity and p_j the phase pressure. The phase mobility can be expressed in terms of the relative permeability $k_{r,j}(S)$ of phase *j*, as follows:

$$\lambda_j(S) = \frac{k_{r,j}(S)\,K}{\mu_j} \tag{2}$$

where μ_j is the viscosity of phase *j*, and *K* the intrinsic saturated permeability of the porous medium. In this sequel, the subscripts *r* and *a* will be used to designate the resin and air phases, respectively.

Assuming incompressibility of the flow, the equations that describe mass conservation for the resin and air phases are given respectively by

$$\nabla\cdot q_r = -\phi\,\frac{\partial S}{\partial t} \quad , \quad \nabla\cdot q_a = -\phi\,\frac{\partial(1-S)}{\partial t} \tag{3}$$

where ϕ denotes the porosity of the fibrous reinforcement. In addition to the conservation of mass and Darcy's law, the pressures of the two phases (resin and air) are related by the capillary pressure function defined as:

$$p_c(S) \;=\; p_a - p_r \tag{4}$$

The basic Eqns. (1)-(3)-(4) can be mathematically manipulated into several alternate multiphase flow formulations with various choices of primary dependent variables. The form of the equations and the choice of the primary variables have considerable implications for the numerical method to be used in the solution of the boundary value problem. There are two main approaches to modeling two-phase flow, arising in the disciplines of hydrology and petroleum engineering: the two pressure formulation and the fractional flow approach.

In the two pressure formulation, the pressure of each phase is chosen as an independent variable and the governing equations are obtained by straightforward substitution of Darcy's equations into the mass balance for each phase in order to eliminate the fluxes. If the air pressure is assumed for sake of simplicity to remain nearly constant, the mass balance equation for the resin phase can thus be solved independently from that of the air phase. The final balance equation obtained in this case reduces to

Richard's equation, which was used in [14] to simulate the injection process in LCM together with van Genuchten capillary pressure function as constitutive equation for saturation [18].

The other formulation used in two-phase flow is the fractional flow approach which originates also from Eqns. (1)-(3)-(4), in which saturation and pressure are chosen as independent variables. In this case the resulting system, known as Buckley-Leverett [19] when capillary pressure is neglected, is composed of the saturation equation

$$\phi \frac{\partial S}{\partial t} + \nabla \cdot \left(q\, f(S) \right) = 0 \tag{5}$$

and the pressure equation

$$\begin{aligned} &\nabla \cdot q = 0 \\ &q = -\lambda\left(S\right) \nabla p \end{aligned} \tag{6}$$

with

$$q = q_r + q_a \quad , \quad \lambda(S) = \lambda_r(S) + \lambda_a(S) \tag{7}$$

called the total velocity and total mobility, respectively. The function *f(S)* in Eqn. (5) is the Buckley–Leverett fractional flow [19] and it will be defined later.

Chui et al. [13] applied this fractional flow approach to predict the distribution of voids in LCM as reported by Lundstrom and Gebart in [20]. However, this formulation cannot replicate the drooping inlet pressure profile observed by Parnas and Phelan [8]. This is believed to be due to the pressure equation, which does not include any sink term [5]. Therefore another form of coupling between the flow and transport equations is needed. In this paper, a new fractional formulation of the flow/transport problem in LCM is proposed to describe the transport of voids and the drooping inlet pressure. Air entrapped at the mesoscale level may be compressed, dissolved and transported with the resin flow, while voids inside the fiber tows are also dissolved and therefore displaced, although in a slower rate [21]. Hence a parameter will be introduced here to separate the mobile and immobile air fractions in the pressure equation.

Two-phase flow formulations require constitutive relations between the capillary pressure, resin saturation and relative permeability to close the boundary value problem. A power law constitutive model between relative permeability and saturation, commonly used in other disciplines, will be considered here:

$$k_{r,r}(S) = k_1\, S^m \quad , \quad k_{r,a}(S) = k_2\, \left(1 - S\right)^m \tag{8}$$

The above parameter m, fitted to experimental data, is related to the pore size and the coefficients k_1 and k_2 are the endpoint relative permeability values of each fluid, which are reached when the other phase, namely resin or air, attains its residual value. Standard choices are linear ($m = 1$) and quadratic ($m = 2$).

3. Proposed mathematical model

In this section, a new fractional flow formulation is introduced with pressure and resin saturation as primary unknowns. Capillary effects are often neglected in LCM, however these are recognized to play an important influence in the process [22]. In the sequel, the basic conservation equations where capillary pressure has been included and the constitutive laws for the two-phase flow models (resin and air) are briefly recalled.

Summing mass conservation equations from Eqn. (3), where velocities are defined by Darcy's law in Eqn. (1), the two-phase flow pressure equation is given by

$$\nabla \cdot Q_t = 0 \quad , \quad Q_t = q_r + q_a = -\left(\lambda_r(S) + \lambda_a(S)\right)\nabla p_r - \lambda_a(S)\nabla p_c \tag{9}$$

Denoting the fractional flow function $f(S)$ and the diffusive coefficient $D_{cf}(S)$ due to capillary effects respectively by

$$\begin{aligned} f(S) &= \frac{\lambda_r(S)}{\lambda_r(S) + \lambda_a(S)} = \frac{k_{r,r}(S)}{k_{r,r}(S) + M\, k_{r,a}(S)} \quad , \\ D_{cf}(S) &= f(S)\, \lambda_a(S) \frac{\partial p_c}{\partial S} \end{aligned} \tag{10}$$

the following expression is derived from Eqn. (9)

$$f(S)\, Q_t = q_r - f(S)\lambda_a(S)\nabla p_c \tag{11}$$

which, combined with mass conservation, leads to the saturation equation for the resin:

$$\phi \frac{\partial S}{\partial t} + \nabla \cdot \left(Q_t\, f(S)\right) = -\nabla \cdot \left(D_{cf}(S)\nabla S\right) \tag{12}$$

In the definition of the fractional flow, M denotes the ratio of viscosity of the wetting phase (resin) over the viscosity of the non wetting phase (air).

Hence, the general flow equations for pressure and saturation including capillary effects become

$$\begin{aligned} &\nabla \cdot \left(\lambda(S)\nabla p_r\right) = -\nabla \cdot \left(\lambda_a(S)\nabla p_c\right) \\ &Q_t = -\lambda(S)\nabla p_r - \lambda_a(S)\nabla p_c \\ &\phi \frac{\partial S}{\partial t} + \nabla \cdot \left(Q_t\, f(S)\right) = -\nabla \cdot \left(D_{cf}(S)\nabla S\right) \end{aligned} \tag{13}$$

The equations governing saturation and pressure are non-linear PDEs strongly coupled through the dependence of the mobility field on saturation in the pressure equation and through the total velocity appearing in the saturation equation. Note also that the capillary pressure p_c appears explicitly in the pressure equation and in the diffusive term of saturation equation. Our goal now is to introduce approximations so as to make the coupling between saturation and pressure/velocity less strong and model void transport.

A new parameter χ is introduced to denote the air fraction which moves with the resin or is dissolved in the resin flow. Hence $(1 - \chi)$ denotes the immobile air fraction, which represents the entrapped residual air in the part and will create the void content after cure. Therefore the mass conservation equations can be rewritten as follows:

$$\begin{aligned} &\nabla \cdot q_r = -\phi \frac{\partial S}{\partial t} \\ &\nabla \cdot \left(\chi q_a\right) = -\phi \frac{\partial\left[\chi(1-S)\right]}{\partial t} \\ &\nabla \cdot \left[(1-\chi) q_a\right] = -\phi \frac{\partial\left[(1-\chi)(1-S)\right]}{\partial t} \end{aligned} \tag{14}$$

Regrouping, Eqn. (14) can be described by similar mass conservation equations:

$$\nabla \cdot \left(q_r + \chi q_a\right) = -\phi \left(1-\chi\right) \frac{\partial S}{\partial t} \tag{15}$$

$$\nabla \cdot \left(q_r + (1-\chi) q_a\right) = -\phi \chi \frac{\partial S}{\partial t} \tag{16}$$

Note that to calculate velocity only the mobile air needs be considered like as Eqn. (15). However, this is not valid to calculate pressure, because it ignores the immobile air fraction. This suggests to add a sink source in the pressure equation like as Eqn. (15). Hence, it is proposed to compute pressure from the following modified equation:

$$\nabla \cdot q_t = -\phi \left(1-\chi\right) \frac{\partial S}{\partial t} \tag{17}$$

and then calculate velocity by taking into account only the mobile air fraction:

$$q_t^{\chi} = q_r + \chi q_a \tag{18}$$

It is natural to assume that air bubbles transported in the flow move at the same velocity as the resin. Therefore the total velocity may be replaced by the following term:

$$q_t^{\chi} = q_r + \chi q_a \approx q_r \left(S + \varphi\left(\chi \frac{k_2}{k_1} M \right)(1-S) \right) = q \tag{19}$$

where φ has been chosen such that the two velocities in Eqn. (19) take the same value for $S = 0$ and $S = 1$ respectively, and $\varphi(1)=1$. For numerical results $\varphi(x) = x^{1/m}$, where m depends on the relative permeability model, and all calculations have been obtained subject to the following conditions:

$$k_1 = 1 \ , \ \ \frac{k_2}{k_1} M = 1 \tag{20}$$

With above assumptions and according to Eqn. (19), when $\chi = 1$, the following total velocity is obtained in Eqn. (17) (where the subscript r for pressure has been omitted):

$$q_t = q_r + q_a \approx q_r \left(S + \varphi(1)(1-S) \right) = q_r(1) = -\frac{K}{\mu_r} k_{r,r}(1) \nabla p \tag{21}$$

Hence, the modified pressure equation (17) can now given by

$$\nabla \cdot \left(\frac{K}{\mu_r} k_1 \nabla p \right) = \phi \, (1-\chi) \frac{\partial S}{\partial t} \tag{22}$$

and the fractional flow formulation to model the process can be summarized as

$$\begin{aligned} &\nabla \cdot \left(\frac{K}{\mu_r} k_1 \nabla p \right) = \phi \, (1-\chi) \frac{\partial S}{\partial t} \\ &q = -\lambda_r \left(\widehat{S} \right) \nabla p \qquad \text{with} \qquad \widehat{S} = S + \varphi(\chi)\,(1-S) \\ &\phi \, \frac{\partial S}{\partial t} + \nabla \cdot \left(q\, f(S) \right) = -\nabla \cdot \left(D_{cf}(S) \nabla S \right) \end{aligned} \tag{23}$$

Note that for $\chi = 1$, which can be interpreted as all air is mobile, Eqn. (22) approximates the pressure equation in conventional two-phase flows when capillary pressure is neglected, which coupled with the saturation equation models the transport of voids [13]. This justifies the introduction of the factor $(1 - \chi)$ in the right hand side of Eqn. (22), whereas that if $\chi = 0$, i.e., if all the air phase is assumed immobile, or when $0 < \chi < 1$, Eqn. (22) introduces the sink source in the pressure equation required to model the experimental dropping of pressure observed in unsaturated flows through dual scale porous media. Note also that the above assumptions result in an expression of the elliptic pressure equation similar to that of the resin phase where the relative permeability used to calculate the velocity has been replaced by $k_{r,r}(\widehat{S})$ with

$$\widehat{S} = S + \varphi(\chi)\,(1-S) \tag{24}$$

The choice of this new saturation is based on two premises. First, the velocity total of the flow is calculated by taking into account only the air fraction which moves with the resin (Eqn. (18)) and, second, the air bubbles transported in the flow move at the same velocity as the resin (Eqn. (19)). Furhtermore, by adjusting the value of parameter χ one can obtain the same effect as when a constant residual air saturation is considered.

The modified pressure equation together with the new expression for the total velocity q will be discretized together with the saturation equation, as it is described by Eqn. (23), to solve the two-phase flow boundary value problem. Finally, to close this system of equations, a constitutive relationship between saturation and relative permeability will be needed as shown in the sequel. The standard boundary conditions of molding problems are used, namely no pressure gradient in the normal direction to the mold wall, specified flow rate at the inlet gate and zero pressure in the empty part of the mold. In summary, the simulation of the filling process involves the following operations at each time step:

1. Use the saturation distribution from the previous step (or initial data) to compute the saturation dependent coefficients in the pressure equation.
2. Calculate the pressure distribution by a standard finite element approximation of the following equation:

$$\nabla \cdot \left(k_1 \nabla p\right) = \frac{\phi\, \mu_r}{K}\left(1-\chi\right)\frac{\partial S}{\partial t} \tag{25}$$

3. Calculate the velocity field from

$$q = -\lambda_r\left(\widehat{S}\right)\nabla p \quad \text{with} \quad \widehat{S} = S + \varphi\left(\chi\right)(1-S) \tag{26}$$

   As described in the previous section, a power law expression for the relative permeability in function of the saturation has been implemented in the numerical simulations.

4. Update the distribution of saturation by integrating equation

$$\phi\,\frac{\partial S}{\partial t} + \nabla \cdot \left(q\, f(S)\right) = -\,\nabla \cdot \left(D_{cf}(S)\nabla S\right) \tag{27}$$

   using a numerical method based on a modified flux limiter technique (see [15] for more details). Here, the fractional flow function $f\,(S)$ and the non-linear diffusive coefficient $D_{cf}(S)$ are given by Eqn. (10).

4. Experimental study

Resin Transfer Molding (RTM) is a composite manufacturing process belonging to the LCM family. It consists of injecting a liquid resin through fibrous reinforcements contained in a rigid mold. In order to test and evaluate the different two-phase flow models devised in this investigation to predict saturation, numerical results will be compared with experimental data. A bidirectional non-crimp fabric (NCF) was selected for this investigation. Fiber properties for this experiment were characterized in [17] and are summarized in table 1.

Weaving pattern	E-glass bidirectional non-crimp fabric (NCF)
Areal weight	517 ± 6 g/m^2
Tow linear weight for warp tows	735 tex
Tow linear weight for weft tows	275 tex
Tow count along warp direction	3.07 tows/cm
Tow count along weft direction	10.31 tows/cm
Number of plies of each preform	6

Table 1. Fiber properties

Unidirectional injection experiments were carried out in a rectangular mold with transparent glass cover. Saturation was evaluated by 2D tomographic reconstruction based on Visible Light Transmission (VLT) [23]. This experimental technique is based on fundamental relationships of optics. It allows a better understanding of the mechanisms of void formation and transport in dual scale fibrous reinforcements (see also [17]). In [17], saturation results are obtained by VLT analysis for an experimental injection carried out at 0.1 ml/s constant flow rate.

The RTM injection was performed at room temperature and atmospheric pressure. The geometry considered is a rectangular mold cavity of 360 mm in length, 105 mm in width and of thickness 3.175 mm. Fig. 1 shows a picture of the mold with its transparent cover and the evolution of the average saturation in time measured at each position along its length. In order to analyze saturation, the flow domain was divided in a grid of 21 by 5 Representative Elementary Volumes (REV) along the length and width respectively. Saturation was evaluated in each REV and an average value was calculated along the width of the piece. Each REV has a dimension of 15 mm by 15 mm. After the inlet port and before the vent, two narrow bands of 22.5 mm long by 105 mm wide were not analyzed.

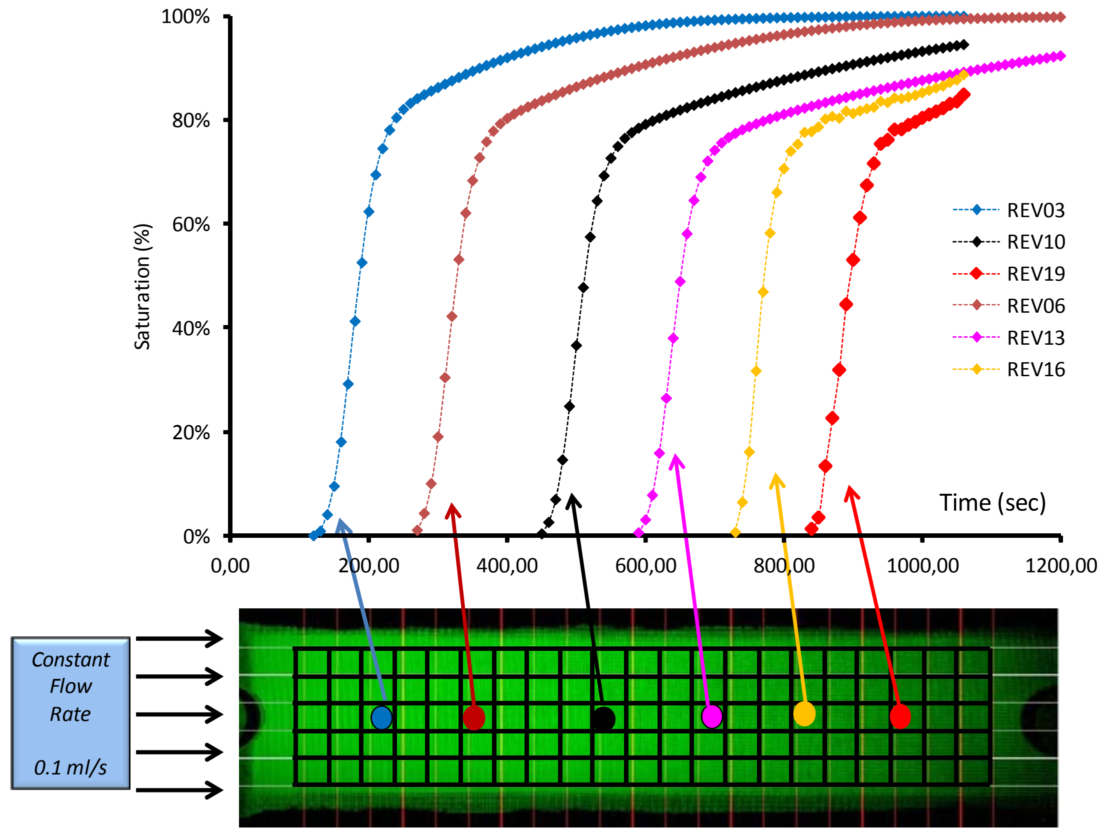

Fig. 1: Schematic representation of experimental saturation for different times analyzed in some REV.

5. Numerical results and discussion

The comparison between experimental and numerical simulations predicting saturation allows investigating the phenomena of void formation and transport during RTM injections. In order to validate the mathematical model proposed in Section 3, numerical results of saturation have been compared with an experimental RTM injection at constant flow rate of 0.1 ml/s. The measured values of the saturated permeability K, of the resin viscosity μ and of porosity ϕ have been set to 7.9 x10^{-10} m^2, 0.4788 Pa.s and 0.614 respectively [17].

The problem has been numerically solved here using the two-phase fractional flow approach described in Section 3 by Eqns. (25)-(27). In these simulations, the diffusive coefficient in the saturation equation has been omitted ($D_{cf} = 0$) and the following values have been used for the parameters:

$$k_1 = 1 \quad , \quad \frac{k_2}{k_1} M = 1 \quad , \quad \chi = 0.32 \qquad (28)$$

The solution uses a finite element method for the elliptic pressure equation coupled with a high order technique to approximate the saturation equation. This last equation belongs to a class of partial differential equations called first order conservation laws which are difficult to solve numerically because they are non-linear and the solutions frequently involve discontinuities. For this purpose, Eqn. (27) for the evolution of saturation has been discretized by using a flux limiter strategy introduced by the authors in [15] to calculate the void fraction in LCM. This technique combines a high order numerical flux in smooth regions with a first order monotonic upwind method in vicinity of discontinuities to avoid the spurious numerical oscillations that would otherwise occur with high order spatial discretisation schemes due to shocks, discontinuities or sharp changes in the solution domain. The flux limiter technique has the ability to limit the extra non physical numerical diffusion introduced by standard first order schemes and it improves significantly the results.

Other of the difficulties encountered in this approximation is connected with the relative permeability, which should be known as a function of saturation. Note that the selection of a model of relative permeability and the values of its parameters can have a significant impact on the predicted saturation, because the flux function of the saturation equation is based on the fractional flow expression which depends of the relative permeability choice.

Figs. 2 and 3 show the comparison between numerical and experimental saturation as a function of time at three different positions along the length of the test mold (REV03, REV10 and REV19). Numerical results for saturation are represented by solid lines while experimental results are depicted by symbols.

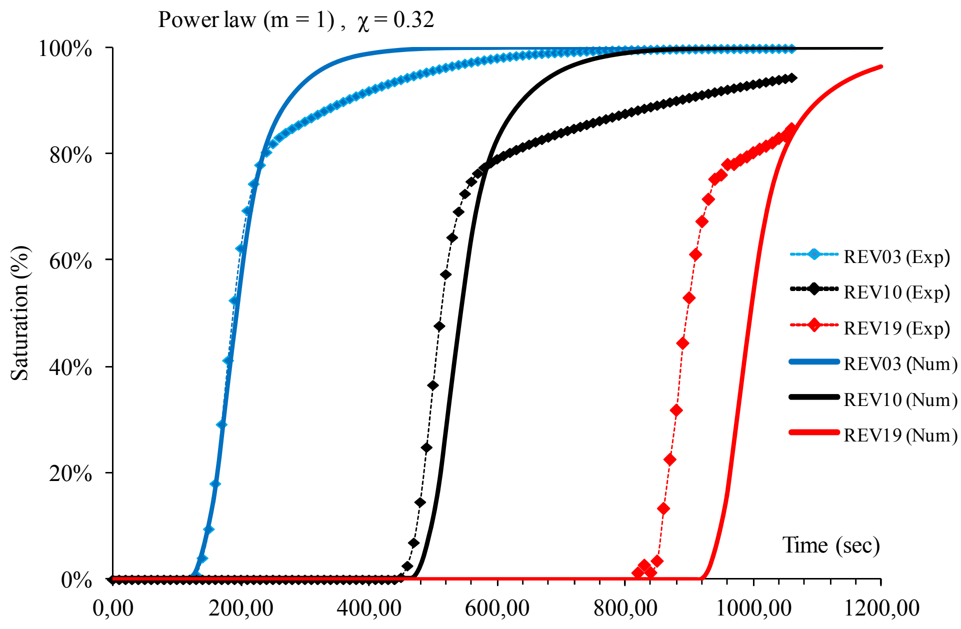

Fig. 2: Comparison between experimental (symbols) and numerical saturation (solid lines) as a function of time for the injection at constant flow of 0.1 ml/s using the two-phase flow formulation given by Eqns. (25)-(27) with a linear power law model for the relative permeability.

For the numerical results of the saturation in Fig. 2 a linear power law model for the relative permeability has been used (Eqn. (8) with m = 1). Hence the mobility in Eqn. (26) has been computed from the following expression

$$k_{r,r}\left(\widehat{S}\right)=\widehat{S} \quad , \quad \widehat{S}=S+\chi(1-S) \tag{29}$$

In this case, with above values for parameters given by Eqn. (28), the resin fractional flow *f(S)* in saturation equation reduces from Eqn. (10) to identity. Note that the linear power law model of relative permeability gives the following saturation equation:

$$\phi\,\frac{\partial S}{\partial t}+\nabla\cdot\left(qS\right)=0 \tag{30}$$

where the degree of saturation is advected with the velocity q. Fig. 2 shows that linear models of relative permeability do not really provide a good match of saturation with experiments. If the flow disturbance of one phase is only due to the restriction of available pore volume caused by the presence of the other fluid, a linear correlation for the relative permeability could be applied. In reality, one phase usually not only influences the flow of another phase just by the restriction in available volume, but also by additional interactions between the fluids. It explains that the quadratic power law model for relative permeability yields better numerical results that the linear power law model, as it can be seen in numerical results in Fig. 3.

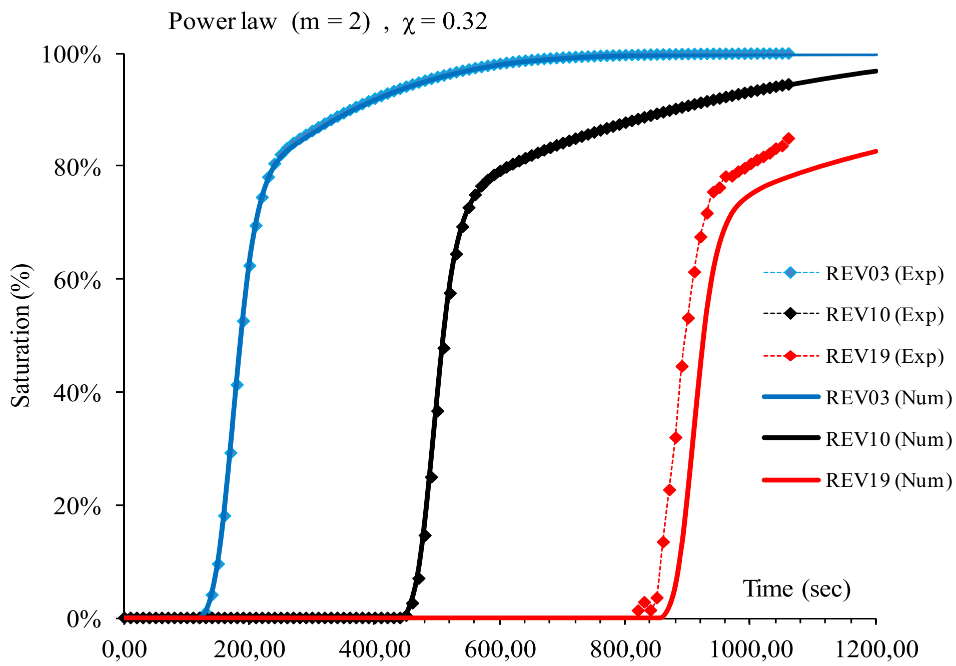

Fig. 3: Comparison between experimental (symbols) and numerical saturation (solid lines) as a function of time for the injection at constant flow of 0.1 ml/s using the two-phase flow formulation given by Eqns. (25)-(27) with a quadratic power law model for the relative permeability.

Numerical results for saturation in Fig. 3 are based on the two-phase flow formulation described in Section 3 by Eqns. (25)-(27), using a quadratic power law model for the relative permeability (Eqn. (8) with $m = 2$). Hence the mobility in Eqn. (26) to simulate the velocity has been computed from the following expression for the relative permeability

$$k_{r,r}\left(\widehat{S}\right) = \widehat{S}^2 \quad , \quad \widehat{S} = S + \chi^{1/2}(1-S) \tag{31}$$

In this case, according to the above assumptions, the saturation equation reduces to

$$\phi \, \frac{\partial S}{\partial t} + \nabla \cdot \left(q \, f(S)\right) = 0 \tag{32}$$

where the resin fractional flow $f(S)$ in the saturation equation have been defined as

$$f(S) = \frac{S^2}{S^2 + (1-S)^2} \qquad (33)$$

It is well known that upwinding is an essential part of any numerical scheme for hyperbolic equations. In our construction of numerical fluxes to compute saturation, the upwind direction has been determined by the sign of the velocity q, calculated from pressure, multiplied by the partial of the fractional flow with respect to resin saturation. Hence, in this case, the saturation is advected with the velocity q multiplied by the slope of the fractional flow curve.

In the first REVs analyzed of Fig. 3 the error is nearly zero. In these cases, only a slight increment in the error measure in the area surrounding the breaking point has been detected. This is related with the flux limiter technique to compute saturation, which automatically changes the scheme from second order to a conventional first order one in the neighborhood of the breaking point. On the other hand, the error increases gradually from REV13 probably because of the flow front has reached the vent location. Hence, the discrepancy between experimental and numerical saturation found in the last curves of Fig. 3 can find its origin in the experimental measurements of the saturation curves.

The model proposed in this paper allows predict saturation in RTM, but this new formulation requires fitting some parameters which depend on the resin injection conditions: k_1 , k_2 , m and χ.

The parameter $\varphi(\chi) = \chi 1/m$ in Eqn. (24) has been taken from experiments as the ratio between the length of the partially saturated region and the total length of the mold at 1200 s, which is the theoretical time required to fill the mold fully saturated for this test.

An important parameter in determining the effectiveness of two phase flow displacement is the endpoint mobility ratio defined as the ratio between the maximum velocity of the displacing fluid (resin) and the maximum velocity of the displaced fluid (air):

$$\frac{\lambda_r(S=1)}{\lambda_a(S=0)} = \frac{k_1}{k_2}\frac{\mu_a}{\mu_r} = \frac{k_1}{k_2 M} \qquad (34)$$

where k_1 is the relative permeability for resin at residual air saturation, meaning that only resin is flowing, while k_2 is the relative permeability for air at irreducible resin saturation, i.e., when only air is flowing. Mobility ratio is directly related to the relative velocity of each fluid. A mobility of one represents equal velocity of the displaced and displacing fluids. In order to secure this last condition we assume Eqn. (20). Optimal numerical results in this paper have been obtained when the endpoint relative permeability for resin k_1 is equal to 1. Hence the relative permeability to air at irreducible resin saturation, k_2 in Eqn. (8), must be relatively low. As can be seen in Fig. 4, the parameter k_1 is very important to decide the correct position of the discontinuity in the resin saturation at the flow front. In order to demonstrate its influence on the numerical predictions a comparison for three different values of k_1 has been showed in Fig 4, where k_2 M = 1 in all cases.

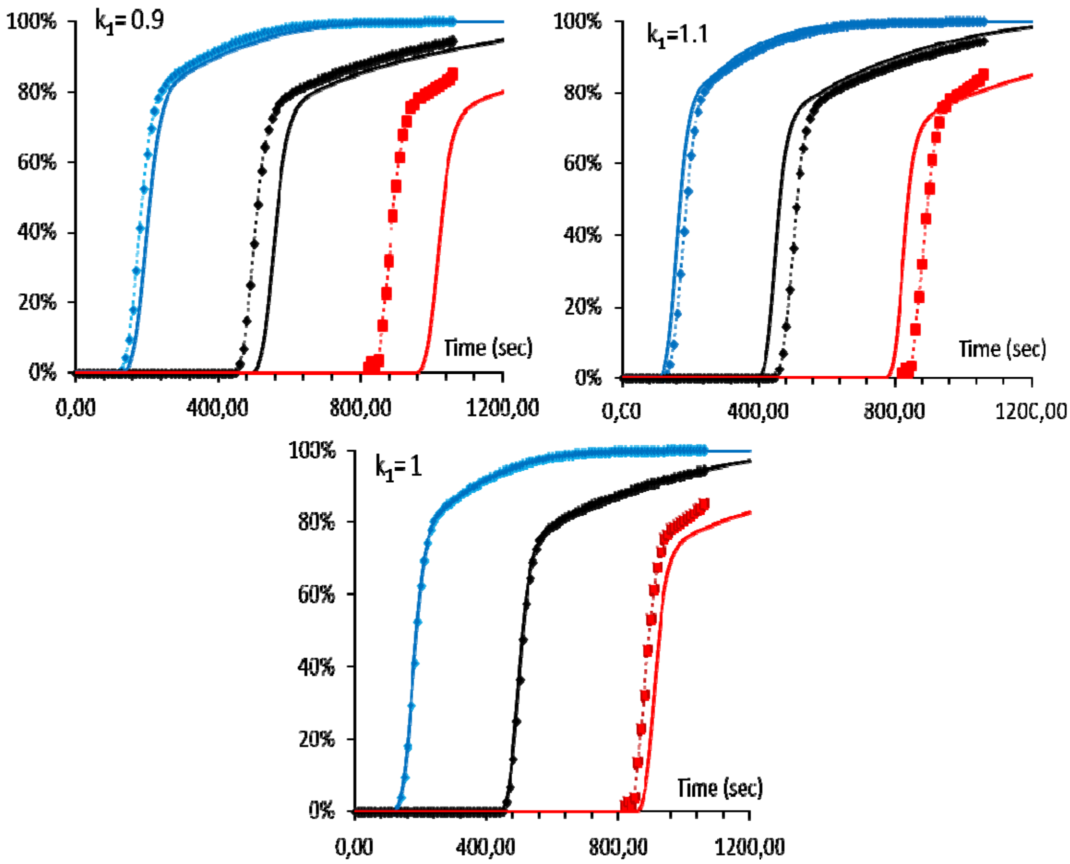

Fig. 4: Comparison between experimental (symbols) and numerical saturation (solid lines) as a function of time for the injection at constant flow of 0.1 ml/s for three different values of k_1.

Other widely used constitutive relations between resin saturation and relative permeability commonly used in petroleum engineering and related fields have been used in numerical simulations, such that Brooks-Corey model [24] generalized from the original Corey model [25] and the van Genuchten-Mualem model [18]. Although numerical results have been omitted in this paper, we note that Brooks-Corey and van Genuchten-Mualem models of relative permeability provide predictions closed to experimental results. However, a slight deviation was observed in these cases near the shock front with numerical results worse than those obtained using a quadratic power law model for relative permeability. In general, in the case of a moderate injection flow rate of 0.1 ml/s, numerical results observed in Fig. 3

show that the two-phase fractional flow model described in Section 3 by Eqns. (25)-(27) provide numerical predictions closed to experimental results. This model uses a quadratic power law of relative permeability and a flux limiter technique [15] to simulate saturation.

Fig. 5 illustrates the inlet pressure (symbols) calculated with the two-phase flow approach, described by Eqns. (25)-(27) using a quadratic power law model of relative permeability. The inlet pressure through a single scale porous medium increases linearly (solid line), whereas it droops with time in dual scale fibrous reinforcements. These numerical results based on the two-phase fractional flow approach described in Section 3 allow demonstrate that the model is not only capable of predicting saturation in RTM, but is also consistent with the drooping pressure observed experimentally in unsaturated flows through dual scale porous media.

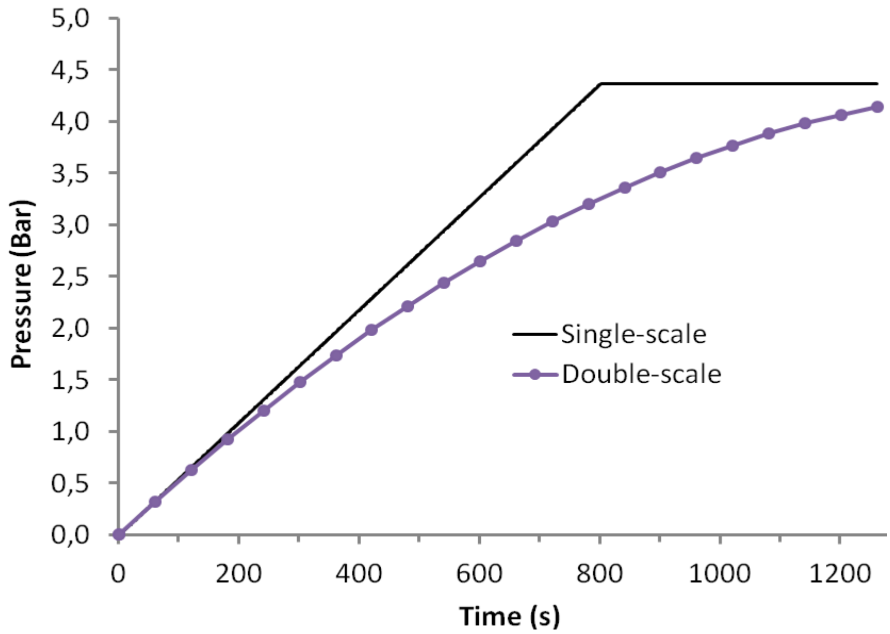

Fig. 5: Numerical inlet pressure during injections at constant flow rate. The linear increase in single scale porous medium (solid line) is compared to the drooping pressure observed in dual scale fibrous reinforcement.

A validation of the proposed model has been done by comparing them with the experimental results for the saturation curves shown in Fig. 13 of Ref. [14]. The experimental curves in [14] was extracted by an image analysis method to determine the saturation curves of a resin/glass fabric system, during infiltration in a transparent mould under constant flow rate. Video acquisitions was transformed by image analysis into saturation level versus position and time, and coupled to inlet pressure measurements. The numerical saturation distribution calculated with the fractional two phase flow described in Section 3 at four filling times of 7.5 s, 10 s, 12.5 s and 17.5 s is depicted in Fig. 6 by solid lines. Experimental results (dashed lines) in Fig. 6 have been extracted from Fig. 13 of Ref. [14]. Numerical results in Fig. 6 correspond to an experimental injection at constant flow rate of 0.00105 m/s and the same conditions described in table 2 of Ref. [14]. Numerical simulations are carried out using the same value for the parameters (k_1 = 1, k_2 M = 1 and m = 2) except for χ which has been set to 0.01. Good agreement was found for saturation between the numerical simulation and the experimental measurements for the four times studied. However, since the parameters depend on the resin injection conditions, optimized parameters for this test could improve numerical results.

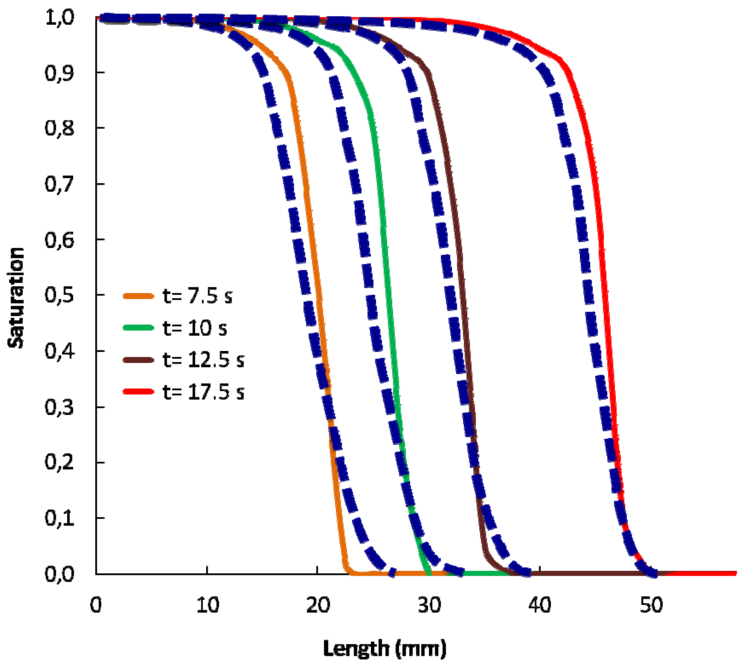

Fig. 6: Experimental (dashed lines) and numerical curves of saturation (solid lines) at different instants for the injection test at constant flow rate of 0.00105 m/s, described in Ref. [14]. Numerical results have been calculated using the two-phase flow formulation given by Eqns. (25)-(27).

6. Conclusion

In order to analyze the formation of voids during resin impregnation in RTM, a new one-dimensional transient solution based on two-phase flow through a porous medium has been devised. The model is based on a fractional two-phase flow formulation with pressure and resin saturation as primary unknowns. After simplification, these equations lead to a system composed of a nonlinear advection-diffusion equation for saturation and elliptic equation for pressure and velocity. The two partial differential equations are coupled by taking into account only the air fraction that moves with the resin in the calculation of velocity and pressure fields.

The two-phase flow model has been implemented to calculate the saturation profiles and compare with experiments for a unidirectional injection in a rectangular mold at 0.1 ml/s injection flow rate. In this approximation, the relative permeability depends on saturation. Models of relative permeability based on a linear power law did not agree as well with experiments as those obtained with a quadratic power law. The quadratic power law for relative permeability model yielded good predictions. In this latter case, not only did numerical and experimental results agree well, but also no correction was required here on the endpoint relative permeability and capillary effects could be neglected in saturation equation.

In this multiphase flow approach, the choice of relative permeability function can have a significant impact on predicted saturation, but also the quality of solution is affected by the numerical method used to solve the saturation equation. Hence, in order to approximate numerically the saturation equation a modified flux limiter technique was used [15]. This method has been coupled with a FEM code for the pressure calculation. The numerical simulations indicate that this approach is sound and provides a good alternative to solve the saturation equation.

Numerical predictions of saturation based on this fractional two-phase flow formulation agree well with experiments for intermediate flow rates, which cover the range of most practical injection conditions. Preliminary validation studies comparing the model with experimental results demonstrate that the model can predict numerical saturation in RTM and the pressure field in dual scale porous media. The next step consists of exploring how the range of application of the two-phase flow model devised in this investigation can be extended to slower and larger injection flow rates.

Acknowledgments: The authors acknowledge financial support of the Spanish Government (Projects DPI2010-20333 and DPI2013-44903-R-AR), of the National Science and Research Council of Canada (NSERC) and of the Canada Reseach Chair (CRC) program.

References

1. Patel N, Lee LJ (1996) Modeling of Void Formation and Removal in Liquid Composite Molding. Part I: Wettability Analysis Polym Compos 17(1): 96-103.

2. Ruiz E, Achim V, Soukane S, Trochu F, Bréard J (2006) Optimization of injection flow rate to minimize micro/macro-voids formation in resin transfer molded composites. Compos Sci Technol 66(3-4): 475-486.

3. Trochu F, Ruiz E, Achim V, Soukane S (2006) Advanced Numerical Simulation of Liquid Composite Molding for Process Analysis and Optimization. Compos Part A: Appl Sci Manufact 37 (6): 890-902.

4. Park CH, Lee W (2011) Modeling void formation and unsaturated flow in liquid composite molding processes: a survey and review. J Reinf Plast Compos 30 (11): 957-977.

5. Pillai KM (2004) Modeling the Unsaturated Flow in Liquid Composite Molding Processes: A Review and Some Thoughts. J Compos Mater 38 (23): 2097-2118.

6. Breard J, Saouab A, Bouquet G (2003) Numerical simulation of void formation in LCM. Compos Part A: Appl Sci Manufact 34: 517- 523.

7. Breard J, Henzel Y, Trochu F, Gauvin R (2003) Analysis of Dynamic Flows through Porous Media. Part I: Comparison between Saturated and Unsaturated Flows in Fibrous Reinforcements. Polym Compos 24(3): 391–408.

8. Parnas RS, Phelan Jr FR (1991) The effect of heterogeneous porous media on mold filling in Resin Transfer Molding. SAMPE Quarterly 22(2): 53–60.

9. Parseval DY, Pillai KM, Advani SG (1997) A simple model for the variation of permeability due to partial saturation in dual scale porous media. Transp Porous Media 27 (3): 243–264.

10. Pillai KM (2002) Governing Equations for Unsaturated Flow through Woven Fiber Mats. Part 1. Isothermal Flows. Compos Part A: Appl Sci Manufact 33(7): 1007–1019.

11. Simacek P, Advani SG (2003) A numerical model to predict fiber tow saturation during Liquid Composite Molding. Compos Sci Technol 63: 1725-1736.

12. García JA, Gascón L, Chinesta F (2010) A flux limiter strategy for solving the saturation equation in RTM process simulation. Compos Part A: Appl Sci Manufact 41:78–82.

13. Chui WK, Glimm J, Tangerman FM, Jardine AP, Madsen JS, Donnellan TM, Leek R (1997) Process Modeling in Resin Transfer Molding as a Method to Enhance Product Quality. SIAM Rev 39(4):714-727.

14. Nordlund M, Michaud V (2012) Dynamic saturation curve measurement for resin flow in glass fibre reinforcement. Compos Part A: Appl Sci Manufact 43: 333-343.

15. García JA, Gascón Ll, Chinesta F (2003) A fixed mesh numerical method for modelling the flow in liquid composites moulding processes using a volume of fluid technique. Comp Methods Appl Mech Engrg 192 (7-8): 877-893.

16. García JA, Gascón Ll, Chinesta F, Trochu F, Ruiz E (2010) An efficient solver of the saturation equation in liquid composite molding processes. Int J Mater Form 3 (2): 1295-1302.

17. Lebel F (2012) Contrôle de la fabrication des composites par injection sur renforts. École Polytechnique de Montréal, Canada.

18. Van Genuchten M Th (1980) Closed-form equation for predicting the hydraulic conductivity of unsaturated soils. Soil Science Soc Am J 44(5): 892-898.

19. Buckley SE, Leverett MC (1942) Mechanism of fluid displacement in sands. Petrol Trans AIME 146: 107-116.

20. Lundstrom TS, Gebart BR (1994) Influence from process parameters on void formation in resin transfer molding. Polym Compos 15(1): 25–33.

21. Lundstrom TS (1997) Measurement of void collapse during resin transfer molding. Compos Part A: Appl Sci Manufact 28 (3): 201-214.

22. Lundstrom TS, Frishfelds V, Jakovics A (2010) Bubble formation and motion in non-crimp fabrics with perturbed bundle geometry. Compos Part A: Appl Sci Manufact 41: 83-92.

23. Lebel F, Fanaei A, Ruiz E, Trochu F (2012) Experimental Characterization by Fluorescence of Capillary Flows in the Fiber Tows of Engineering Fabrics. Open Journal of Inorganic Non-Metallic Materials 2(3): 25-45.

24. Brooks RH, Corey AT (1964) Hydraulic properties of porous media. Colorado State University. Hydrology Papers 1-37.

25. Corey AT (1954) The Interrelation Between Gas and Oil Relative Permeabilities. Producers Monthly 19 (1): 38–41.